




# Faster Construction of a Planar Distance Oracle with $\tilde{O}(1)$ Query Time

Itai Boneh   

University of Haifa, Israel

Reichman University, Herzliya, Israel

Shay Golan   

University of Haifa, Israel

Reichman University, Herzliya, Israel

Shay Mozes  

Reichman University, Herzliya, Israel

Daniel Prigan  

Reichman University, Herzliya, Israel

Oren Weimann  

University of Haifa, Israel

---

## Abstract

We show how to preprocess a weighted undirected  $n$ -vertex planar graph in  $\tilde{O}(n^{4/3})$  time, such that the distance between any pair of vertices can then be reported in  $\tilde{O}(1)$  time. This improves the previous  $\tilde{O}(n^{3/2})$  preprocessing time [JACM'23].

Our main technical contribution is a near optimal construction of *additively weighted Voronoi diagrams* in undirected planar graphs. Namely, given a planar graph  $G$  and a face  $f$ , we show that one can preprocess  $G$  in  $\tilde{O}(n)$  time such that given any weight assignment to the vertices of  $f$  one can construct the additively weighted Voronoi diagram of  $f$  in near optimal  $\tilde{O}(|f|)$  time. This improves the  $\tilde{O}(\sqrt{n|f|})$  construction time of [JACM'23].

**2012 ACM Subject Classification** Theory of computation  $\rightarrow$  Data structures design and analysis

**Keywords and phrases** Distance Oracle, Planar Graph, Construction Time

**Digital Object Identifier** 10.4230/LIPIcs.ICALP.2025.33

**Category** Track A: Algorithms, Complexity and Games

**Related Version** *Full Version*: <https://arxiv.org/abs/2503.18425> [2]

**Funding** Israel Science Foundation grant 810/21.

## 1 Introduction

In this paper we investigate the following question: *How fast can you preprocess a planar graph so that subsequent distance queries can be answered in near-optimal  $\tilde{O}(1)$  time?* Imagine you could do the preprocessing in near-optimal  $\tilde{O}(n)$  time. This would be truly remarkable, since it would allow us to efficiently convert between standard graph representations, which support quick local (e.g., adjacency) queries, into a representation that supports quick non-local distance queries. In a sense, this can be thought of as an analogue for distances of the Fast Fourier Transform (which converts in  $\tilde{O}(n)$  time between the time domain and the frequency domain). Such a tool would allow us to develop algorithms for planar graphs that can access any pairwise distance in the graph essentially for free! Unfortunately, we are still far from obtaining  $\tilde{O}(n)$  preprocessing time. The fastest preprocessing time is  $\tilde{O}(n^{3/2})$  [9]. We make a step in this direction by improving the preprocessing time to  $\tilde{O}(n^{4/3})$  in weighted undirected planar graphs.



© Itai Boneh, Shay Golan, Shay Mozes, Daniel Prigan, and Oren Weimann;  
licensed under Creative Commons License CC-BY 4.0

52nd International Colloquium on Automata, Languages, and Programming (ICALP 2025).

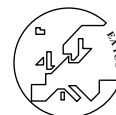
Editors: Keren Censor-Hillel, Fabrizio Grandoni, Joël Ouaknine, and Gabriele Puppis

Article No. 33; pp. 33:1–33:21



Leibniz International Proceedings in Informatics

LIPICs Schloss Dagstuhl – Leibniz-Zentrum für Informatik, Dagstuhl Publishing, Germany



Formally, a *distance oracle* is a data structure that can report the distance  $\text{dist}(u, v)$  between any two vertices  $u$  and  $v$  in a graph  $G$ . Distance oracles for planar graphs have been studied extensively in the past three decades both in the exact [1, 4, 9, 10, 13–15, 17, 19, 21, 26, 32, 36, 38, 40] and in the approximate [8, 22–25, 29, 39, 41] settings. In the approximate setting, Thorup [39] presented a near-optimal oracle that returns  $(1 + \varepsilon)$ -approximate distances (for any constant  $\varepsilon$ ) in  $\tilde{O}(1)$  time and requires  $\tilde{O}(n)$  space and construction time (see also [8, 22–25, 29, 41] for polylogarithmic improvements). Is it possible that the same near-optimal bounds can be achieved without resorting to approximation? We next review the rich history of *exact* oracles in planar graphs.

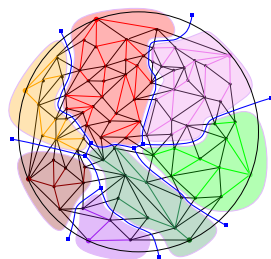
**The history of exact planar distance oracles.** Let  $Q$  and  $S$  denote the query-time and the space of an oracle, respectively. The early planar distance oracles [1, 13, 15] were based solely on *planar separators* [18, 31, 33] and achieved a tradeoff of  $Q = \tilde{O}(n/\sqrt{S})$  for  $S \in [n^{4/3}, n^2]$ , and  $Q = O(n^2/S)$  for  $S \in [n, n^{4/3}]$ . In [17], Fakcharoenphol and Rao introduced the use of *Monge matrices* to distance oracles, and devised an oracle with  $\tilde{O}(n)$  space and  $\tilde{O}(\sqrt{n})$  query time. By combining their ideas with Klein’s [6, 25] *multiple source shortest path* (MSSP) data structure, Mozes and Sommer [36] obtained the  $Q = \tilde{O}(n/\sqrt{S})$  tradeoff for nearly the full range  $[n \log \log n, n^2]$ . Other works [19, 36, 38, 40] focused on achieving strictly optimal query-time *or* strictly optimal space. Namely, Wulff-Nilsen’s work [40] gives optimal  $O(1)$  queries with weakly subquadratic  $O(n^2 \log^4 \log n / \log n)$  space, whereas Nussbaum [38] and Mozes and Sommer’s [36] oracles give optimal  $O(n)$  space with  $O(n^{1/2+\epsilon})$  query-time. Except for [40], all of the above oracles can be constructed in  $\tilde{O}(n)$  time. However, none of them provides polylogarithmic  $\tilde{O}(1)$  query-time using truly subquadratic  $O(n^{2-\epsilon})$  space.

In FOCS 2017, Cohen-Addad, Dahlgaard, and Wulff-Nilsen [14] (inspired by Cabello’s [5] breakthrough use of *Voronoi diagrams* for computing the diameter of planar graphs) realized that Voronoi diagrams, when applied to regions of an  $r$ -division, can be used to break the barrier mentioned above. In particular, they presented the first oracle with  $\tilde{O}(1)$  query-time and truly subquadratic  $O(n^{5/3})$  space, or more generally, the tradeoff  $Q = \tilde{O}(n^{5/2}/S^{3/2})$  for any  $S \in [n^{3/2}, n^{5/3}]$ . This came at the cost of increasing the preprocessing time from  $\tilde{O}(n)$  to  $O(n^2)$ , which was subsequently improved to match the space bound [20]. In SODA 2018, Gawrychowski, Mozes, Weimann, and Wulff-Nilsen [21] improved the space and preprocessing time to  $\tilde{O}(n^{3/2})$  with  $\tilde{O}(1)$  query-time (and the tradeoff to  $Q = \tilde{O}(n^{3/2}/S)$  for  $S \in [n, n^{3/2}]$ ) by defining a dual representation of Voronoi diagrams and developing an efficient *point-location* mechanism on top of it. In STOC 2019, Charalampopoulos, Gawrychowski, Mozes, and Weimann [10] observed that the same point-location mechanism can be used on the Voronoi diagram for the complement of regions in the  $r$ -division. This observation alone suffices to improve the oracle size to  $O(n^{4/3})$  (while maintaining  $\tilde{O}(1)$  query-time). By combining this with a sophisticated recursion (where a query at recursion level  $i$  reduces to  $\log n$  queries at level  $i + 1$ ) they further obtained an oracle of size  $n^{1+o(1)}$  and query-time  $n^{o(1)}$ . Finally, in SODA 2021, Long and Pettie [32] showed how much of the point-location work can be done without recursion, and that only two (rather than  $\log n$ ) recursive calls suffice. This led to the state of the art oracle, requiring  $n^{1+o(1)}$  space and  $\tilde{O}(1)$  query-time or  $\tilde{O}(n)$  space and  $n^{o(1)}$  query-time.<sup>1</sup>

In terms of space and query time, these latter Voronoi-based oracles are almost optimal. However, their construction time is  $\tilde{O}(n^{3/2})$ , and improving it is mentioned in [9] as an important open problem. The bottleneck behind this  $\tilde{O}(n^{3/2})$  bound is the time for constructing Voronoi diagrams as we next explain.

<sup>1</sup> A journal version containing all the above Voronoi-based oracles was published in JACM in 2023 [9].

**Point-location in Voronoi diagrams.** Let  $X$  be a planar graph, and let  $f$  be a face of  $X$ . The vertices of  $f$  are called the *sites* of the Voronoi diagram, and each site  $s$  has a weight  $\omega(s) \geq 0$  associated with it. The distance between a site  $s$  and a vertex  $v \in X$ , denoted by  $\text{dist}^\omega(s, v)$  is defined as  $\omega(s)$  plus the length of the  $s$ -to- $v$  shortest path in  $X$ . The *additively weighted Voronoi diagram*  $\text{VD}(f, \omega)$  is a partition of  $X$ 's vertices into pairwise disjoint sets, one set  $\text{Vor}(s)$  for each site  $s$ . The set  $\text{Vor}(s)$ , called the *Voronoi cell* of  $s$ , contains all vertices in  $X$  that are closer (w.r.t.  $\text{dist}^\omega(\cdot, \cdot)$ ) to  $s$  than to any other site (we assume that distances are unique to avoid the need to handle ties<sup>2</sup>). A *point-location* query  $v$  asks for the site  $s$  whose Voronoi cell  $\text{Vor}(s)$  contains  $v$ . There exists a dual representation  $\text{VD}^*(f, \omega)$  of  $\text{VD}(f, \omega)$ . The size of this representation is  $O(|f|)$ , and together with an MSSP data structure it supports point-location queries in  $\tilde{O}(1)$  time.



■ **Figure 1** A graph (piece)  $X$ . The vertices of  $X$ 's infinite face  $f$  are the sites of the Voronoi diagram  $\text{VD}$ . Each site is represented by a unique color, which is also used to shade its Voronoi cell. The dual representation  $\text{VD}^*$  is illustrated as the blue tree. The tree has 7 leaves (corresponding to 7 copies of  $f^*$ ) and 5 internal nodes (corresponding to the 5 trichromatic faces of  $\text{VD}$ ). The edges of the tree correspond to contracted subpaths in  $X^*$ .

**Our results and techniques.** In [9], it was shown that given the MSSP of a graph (piece)  $X$ , a face  $f$  of  $X$ , and additive weights  $\omega(\cdot)$  to the vertices of  $f$ , the Voronoi diagram  $\text{VD}^*(f, \omega)$  can be constructed in  $\tilde{O}(\sqrt{n|f|})$  time. In this paper, we show (see Theorem 15) how to construct it in near-optimal  $\tilde{O}(|f|)$  time when the graph is undirected. As discussed below, this leads to a static distance oracle of space  $\tilde{O}(n^{4/3})$ , construction time  $\tilde{O}(n^{4/3})$ , and query-time  $\tilde{O}(1)$ . In addition, it implies a *dynamic* distance oracle that supports  $\tilde{O}(1)$ -time distance queries from a single-source  $s$ , and  $\tilde{O}(n^{2/3})$ -time updates consisting of edge insertions, edge deletions, and changing the source  $s$ . The dynamic distance oracle is obtained by simply plugging our construction into the oracle of Charalampopoulos and Karczmarz [12] (thus improving its update time from  $\tilde{O}(n^{4/5})$  to  $\tilde{O}(n^{2/3})$ ). We note that the current best *all-pairs* dynamic oracle by Fakcharoenphol and Rao [17] has  $\tilde{O}(n^{2/3})$  update time and  $\tilde{O}(n^{2/3})$  query time. Therefore, in undirected graphs, our new oracle achieves the same bounds but has the benefit that, between source changes, the query takes only  $\tilde{O}(1)$  time.

Our construction is inspired by Charalampopoulos, Gawrychowski, Mozes, and Weimann who showed in ICALP 2021 [11] that near-optimal  $\tilde{O}(|f|)$  construction time is possible for the special case when the planar graph is an *alignment graph* of two strings. The alignment graph is an acyclic grid graph of constant degree. More importantly, shortest paths in this graph are monotone, in the sense that they only go right or down along the grid. This makes the Voronoi diagram of every piece  $X$  much more structured. In particular, one can find

<sup>2</sup> This assumption can be achieved in  $O(n)$  time. With high probability using [34, 37], or deterministically using [16].

the trichromatic vertices of  $VD^*$  (i.e., the faces of  $X$  whose vertices belong to three different Voronoi cells) by recursively zooming in on them using cycle separators; The intersection of a cycle separator with each Voronoi cell consists of at most two contiguous intervals of the cycle separator. This partition induced by these intervals can be found with a binary search approach, whose complexity (up to a logarithmic factor) is linear in the number of trichromatic vertices enclosed by the cycle. From the partition it is easy to deduce whether a trichromatic vertex of  $VD^*$  is enclosed by the cycle separator, and infer whether we should recurse on each side of the separator. In this paper we extend this binary search approach to general undirected planar graphs.

At a first glance, such an extension seems impossible as the intersection of cycle separators and Voronoi cells might be very fragmented, even when there are only three sites. To overcome this, we use *shortest path separators*. Such separators have been widely used in essentially all approximate distance oracles for planar graphs, but also in exact algorithms (e.g., [3, 7, 28, 35]). These cycle separators may contain  $\Theta(n)$  edges (rather than  $O(\sqrt{n})$ ), but consist of two shortest paths  $P, P'$ , so that, because the graph is undirected, any other shortest path can intersect each of  $P, P'$  at most once. In our context, this implies a monotonicity property when we restrict our attention to shortest paths that enter the cycle separator only from the left or only from the right. If we only allow paths to enter  $P$  from one side, say the left, then the intersection of each Voronoi cell (with distances now defined under this restriction) with  $P$  is a single contiguous interval.

To better explain the difficulties with this approach and how we overcome them, let us first define some terminology. We say that vertex  $v \in P$  *prefers* a site  $s$  if  $v$  belongs to  $\text{Vor}(s)$  (defined without any restrictions). We say that  $v \in P$  *left-prefers* a site  $s$  if  $v$  belongs to  $\text{Vor}(s)$  under the restriction that paths are only allowed to enter  $P$  from the left. Repeating the above discussion using this terminology, the partition induced by the prefers relation may be very fragmented, but the partition induced by the left-prefers relation is not fragmented. There are two immediate problems with working with the partition induced by left-preference (or right-preference). First, we are interested in constructing the Voronoi diagram without any restrictions, and second, we do not know how to efficiently compute shortest paths under restrictions on the direction in which they enter  $P$ .

To address the first difficulty we show that one can infer which sides of the cycle separator contain a trichromatic vertex of the Voronoi diagram (without restrictions) by inspecting the endpoints of the intervals of the two partitions - the one with respect to left-preference and the one with respect to right-preference. This is shown in Section 4. We also show, by adapting the divide-and-conquer construction algorithm of [20], how to reduce the problem of computing a Voronoi diagram with many sites to the problem of computing the trichromatic vertex of a Voronoi diagram with only three sites. This is explained in Section 5.

Overcoming the second difficulty is the heart of our technical contribution. We know how to efficiently determine, by enhancing the standard MSSP data structure, whether the true shortest path from a site  $s$  to a vertex  $v \in P$  enters  $P$  from the right or from the left. However, we do not know how to efficiently report the shortest path from  $s$  to  $v$  that enters  $P$  from the other side (because that path is not the overall shortest path from  $s$  to  $v$ ). We observe that we can work with *relaxed* preferences. If  $v$  prefers  $s$  (without restrictions on left/right), then: (1) we might as well say that  $v$  both right-prefers and left-prefers  $s$  (because either way this will point us to  $s$ ), and (2) if the shortest path from  $s$  to  $v$  enters  $P$  from the right, we do not really care what the left preference of  $v$  is, so we might as well say that  $v$  left-prefers  $s'$  for any site  $s'$ . In Section 3 we describe how to compute a partition with respect to such a relaxed notion of left-preference and right-preference. The exact details are a bit more complicated than described here. In particular we use the term *like* rather than *prefer* to express that the preference is more loose.

Constructing a partition with relaxed preferences turns out to be more complicated than with strict preferences. One challenge comes from the fact that with relaxed preferences making progress in a binary search procedure is problematic. This is because a vertex  $v$  of  $P$  no longer has a unique left-preferred site  $s$ . In fact, when working with relaxed preferences, a vertex  $v$  may equally like all sites. Thus, we need to have some way to recognize a “winner” site with respect to a vertex that does not have a unique preference. Another challenge we encounter is what we call *swirly* paths - when the  $s$ -to- $v$  path goes around  $P$  before entering  $P$ . Swirly paths make the realizations of many of the arguments outlined here more complicated. The structure of the shortest paths that allows us to make progress in the binary search procedure is different and more complicated in the presence of swirly paths. Moreover, we do not always know how to efficiently identify whether a shortest path is swirly or not. To simplify the presentation we first explain how to obtain a partition with respect to relaxed preferences when there are no swirly paths. In the full version of the paper [2] we describe how to handle swirly paths.

We believe that our result is a promising step toward exact oracles that simultaneously have optimal space, query-time and preprocessing time. One way to achieve this would be to be able to find a way to use recursion to obtain the functionality of our enhanced MSSP data structure without actually computing it over and over in large regions of the graph, in a similar manner to the way this issue was avoided for the standard MSSP in [9]). This seems to be the only significant obstacle preventing us from pushing our new ideas all the way through, and obtaining an almost optimal  $n^{1+o(1)}$  construction time for undirected planar graphs.

## 2 Preliminaries

**Representation of Voronoi diagrams.** With a standard transformation (without increasing the size of  $G$  asymptotically) we can guarantee that each vertex of  $G$  has constant degree and that  $G$  is triangulated. Consider a subgraph  $X$  (called a *piece*) of  $G$  whose boundary vertices  $\partial X$  (vertices incident to edges in  $G \setminus X$ ) lie on a single face  $f$  of  $X$ . Note that  $f$  is the only face of  $X$  that is not a triangle. The vertices of  $f$ , assigned with weights  $\omega(\cdot)$ , are the sites of the Voronoi diagram  $\text{VD} = \text{VD}(f, \omega)$  of  $X$ . There is a dual representation  $\text{VD}^*$  of  $\text{VD}$  as a tree with  $O(|f|)$  vertices (see Figure 1): Let  $X^*$  be the planar dual of  $X$ . Consider the subgraph of  $X^*$  consisting of the duals of edges  $uv$  of  $X$  such that  $u$  and  $v$  are in different Voronoi cells. In this subgraph, we repeatedly contract edges incident to degree-2 vertices. The remaining vertices (edges) are called *Voronoi vertices (edges)*. A Voronoi vertex is dual to a face whose three vertices belong to three different Voronoi cells. We call such a face (and its corresponding dual vertex) *trichromatic*. Finally, we define  $\text{VD}^*$  to be the tree obtained from the subgraph by replacing the node  $f^*$  by multiple copies, one for each edge incident to  $f^*$ . The complexity (i.e., the number of vertices and edges) of  $\text{VD}^*$  is  $O(|f|)$ . For example, in a  $\text{VD}$  of just two sites  $s$  and  $t$ , there are no trichromatic faces. In this case,  $\text{VD}^*$  is just a single edge corresponding to an  $st$ -cut or equivalently to a cycle in the dual graph. We call this cycle the *st-bisector* and denote it by  $\beta^*(s, t)$ . Note that a trichromatic vertex is a meeting point of three bisectors. Another important example is a  $\text{VD}$  of three sites (we call this a *trichromatic VD*). Such a  $\text{VD}$  has at most one trichromatic face (in addition to face  $f$  itself).

**Using point-location for distance oracles.** To see why point-location on Voronoi diagrams is useful for distance oracles, we describe here the  $\tilde{O}(n^{4/3})$ -space  $\tilde{O}(1)$ -query oracle of [10] that we will be using. It begins with an  $r$ -division of the graph  $G$ . This is a partition of  $G$

into  $O(n/r)$  subgraphs (called *pieces*) such that every piece  $X$  contains  $O(r)$  vertices and  $O(\sqrt{r})$  boundary vertices  $\partial X$  (vertices shared by more than one piece). An  $r$ -division can be computed in  $\tilde{O}(n)$  time [27] with the additional property that the boundary vertices  $\partial X$  of every piece  $X$  lie on a constant number of faces of the piece (called *holes*). To simplify the presentation, we assume that  $\partial X$  lies on a single hole (in general, we apply the same reasoning to each hole separately, and return the minimum distance found among the  $O(1)$  holes). The oracle consists of the following for each piece  $X$  of the  $r$ -division:

1. The  $O(|X|^{3/2})$  space,  $O(|X|^{3/2})$  construction time,  $\tilde{O}(1)$  query-time distance oracle of [21] on the graph  $X$ . In total, these require  $O(n\sqrt{r})$  space and construction time.
2. Two MSSP data structures [25], one for  $X$  and one for  $X^{out} = G \setminus (X \setminus \partial X)$ , both with sources  $\partial X$ . The MSSP for  $X$  requires space  $O(r \log r)$ , and the MSSP for  $X^{out}$  requires space  $O(n \log n)$ . Using these MSSPs, we can then query in  $\tilde{O}(1)$  time the  $u$ -to- $v$  distance for any  $u \in \partial X$  and  $v \in G$ . The total space and construction time of these MSSPs is  $\tilde{O}(n^2/r)$ , since there are  $O(n/r)$  pieces.
3. For each vertex  $u$  of  $X$ , compute the Voronoi diagram  $\text{VD}_{in}(u, X)$  (resp.  $\text{VD}_{out}(u, X)$ ) for  $X$  (resp.  $X^{out}$ ) with sites  $\partial X$  and additive weights the distances from  $u$  to these vertices in  $G$  (the additive weights are computed in  $\tilde{O}(|\partial X|) = \tilde{O}(\sqrt{r})$  time using [17]). Each Voronoi diagram can be represented in  $O(\sqrt{r})$  space [21] and can be constructed in  $\tilde{O}(\sqrt{n\sqrt{r}})$  time [10]. Hence, all Voronoi diagrams require  $O(n\sqrt{r})$  space and  $\tilde{O}(n^{3/2}r^{1/4})$  construction time.

To query a  $u$ -to- $v$  distance, let  $X$  be the piece that contains  $u$ . If  $v \notin X$  then the  $u$ -to- $v$  path must cross  $\partial X$ . We perform a point-location query for  $v$  in  $\text{VD}_{out}(u, X)$  in time  $\tilde{O}(1)$  [21]. If  $v \in \text{Vor}(s)$  then we return the  $u$ -to- $s$  distance (from the precomputed additive weight) plus the  $s$ -to- $v$  distance (from the MSSP of  $X^{out}$ ). Otherwise,  $v \in X$  and we return the minimum of two options: (1) The shortest  $u$ -to- $v$  path crosses  $\partial X$ . This is similar to the previous case except that the point-location query for  $v$  is done in  $\text{VD}_{in}(u, X)$ . (2) The shortest  $u$ -to- $v$  path does not cross  $\partial X$  (i.e., the path lies entirely within  $X$ ). We retrieve this distance by querying the distance oracle stored for  $X$ .

By choosing  $r = n^{2/3}$  we get an oracle of space  $\tilde{O}(n^{4/3})$  and query-time  $\tilde{O}(1)$ . The construction time however is  $\tilde{O}(n^{5/3})$ . Notice that the only bottleneck preventing  $\tilde{O}(n^{4/3})$  construction time is the construction of the Voronoi diagrams.

**Shortest path separators.** A *shortest path separator*  $Q$  is a balanced cycle separator consisting of two shortest paths  $P$  and  $P'$  (emanating at the same vertex) plus a single edge. A complete recursive decomposition tree  $T$  of  $G$  using shortest path separators can be obtained in linear time [30].

An arc  $e = uv$  emanates (enters) left of a simple path  $P$  if there exist two arcs  $e_1, e_2$  in  $P$ , such that  $u$  ( $v$ ) is the head of  $e_1$  and the tail of  $e_2$ , and  $e$  appears between  $e_1$  and  $e_2$  in the clockwise order of arcs incident to  $u$ . Otherwise,  $e$  emanates (enters) right of  $P$ . Notice that this is not defined for the endpoints of  $P$ , however, in the context in which we will use it, we will always extend  $P$  so that its original endpoints will become internal. Specifically, consider a shortest path separator  $Q$  composed of an  $x$ -to- $y$  path  $P$ , an  $x$ -to- $y'$  path  $P'$ , and an edge  $(y, y')$ . Then, we will extend  $P$  on one side with  $y'$  and on the other side with the vertex following  $x$  on  $P'$ . A symmetric extension will be done for  $P'$ .



### 3 Efficient Computation of a Relaxed Partition

In this section we define a relaxed partition, and show how to compute it in  $\tilde{O}(1)$  time.

#### 3.1 Definitions and data structures

In our settings, let  $F$  denote the face, and let  $H \subseteq F$  denote a subset of vertices (sites) of  $F$  (for the most part, we will use  $|H| = 3$  in order to find trichromatic faces, see Section 4). We say that vertex  $v \in P$  *prefers* a site  $c \in H$  if  $v$  belongs to  $\text{Vor}_H(c)$ . It is natural to partition the vertices of  $P$  according to the site in  $H$  that they prefer. In the case of the alignment graph of [11], each part in this partition is a contiguous interval of  $P$ . In general planar graphs however, this is not the case, and the parts can be very fragmented.

We observe that the partition would induce contiguous intervals if we only consider shortest paths that are allowed to enter  $P$  from the right (or only from the left). In that case we can say that a vertex  $v \in P$  *right-prefers* (left-prefers)  $c$ . We know how to determine efficiently whether the true shortest path from a site  $c$  to a vertex  $v \in P$  enters  $P$  from the right or from the left. But the problem is that then we do not know how to efficiently report the shortest path from  $c$  to  $v$  that enters  $P$  from the other side (because it is not the overall shortest path from  $c$  to  $v$ ).

To overcome this issue we observe that we can work with relaxed preferences, which we call *like*. If  $v$  prefers  $c$  (without restrictions on left/right), then we might as well say that  $v$  both right-likes and left-likes  $c$  (because either way this will point us to  $c$ ). Similarly, if  $v$  prefers  $c$  (again, without restrictions on left/right) then if the shortest path from  $c$  to  $v$  enters  $P$  from the right, we do not really care what the left like of  $v$  is (since in this case shortest paths entering  $P$  from the left are just irrelevant), so we may as well say that  $v$  left-likes  $c'$  for any site  $c'$ .

Recall that the endpoints of  $P$  are  $x$  and  $y$ . We denote by  $s_x$  and  $s_y$  the sites of  $H$  such that  $x \in \text{Vor}_H(s_x)$  and  $y \in \text{Vor}_H(s_y)$ . In practice we will use the left-like (and symmetrically the right-like) relation with respect to a subset  $S \subseteq H$  of sites. If the true site in  $S \cup \{s_x, s_y\}$  that  $v$  prefers (without restrictions on left/right) is not one of the sites in  $S$  then we may as well say that  $v$  both left-likes and right-likes all sites in  $S$  because eventually they will have no effect on the true answer.

The following definition formalizes the above discussion.

► **Definition 1** (( $S$ , left)-like). *Let  $P$  be an  $x$ -to- $y$  shortest path, let  $H = \{h_1, h_2, \dots, h_{|H|}\}$  be a cyclic subsequence of a face  $F$ , and let  $S = \{s_1, s_2, \dots, s_{|S|}\}$  be a subsequence of  $H$ . Let  $s_x \in H$  (resp.  $s_y$ ) be the site such that  $x \in \text{Vor}_H(s_x)$  (resp.  $y \in \text{Vor}_H(s_y)$ ). A vertex  $v \in P$  that belongs to the Voronoi cell  $\text{Vor}_{S \cup \{s_x, s_y\}}(c)$  is said to ( $S$ , left)-like  $s_i$  if at least one of the following holds: (1)  $c = s_i$ , (2) the shortest path from  $c$  to  $v$  enters  $P$  from the right, or (3)  $c \notin S$ .*

This notion of ( $S$ , left)-like, induces a *relaxed partition* of  $P$ , in which the parts do form contiguous intervals along  $P$ . The relaxed partition has the property that for every  $v \in P$  if  $v \in \text{Vor}_H(c)$  and  $c$  reaches  $P$  from some *direction* (left or right) then in the ( $H$ , *direction*)-relaxed partition  $v$  is in the part of  $P$  corresponding to site  $c$ . In other words, together, the ( $H$ , left) and ( $H$ , right)-relaxed partitions assign to each vertex of  $P$  at most two sites in  $H$ , and it is guaranteed that one of these two sites is the true site of  $v$ .

► **Definition 2** (Relaxed Partition). *Let  $P$  be a shortest path, and let  $S$  and  $H$  be cyclic subsequences of a face  $F$  with  $S \subseteq H$ , denoted by  $S = \{s_1, s_2, \dots, s_{|S|}\}$  and  $H = \{h_1, h_2, \dots, h_{|H|}\}$ .*

A relaxed  $(S, \text{left})$ -partition of  $P$  w.r.t.  $S$  is a partition of  $P$  into  $|S|$  disjoint subpaths  $P_i = P[u_i, v_i]$  such that every  $x \in P_i$  is a vertex that  $(S, \text{left})$ -likes  $s_i$ .

The definitions of  $(S, \text{right})$ -like and of an  $(S, \text{right})$ -relaxed partition are symmetric. The main part of our algorithm is dedicated to finding a relaxed partition. First, in Section 3.3 we will show how to find a relaxed partition of  $P$  w.r.t.  $S \subset H$  consisting of only two sites. Then, in Section 3.4, we explain how to obtain a relaxed partition of  $P$  w.r.t.  $H$  by combining the relaxed partitions of pairs of sites in  $H$ .

For two vertices  $u, v$  we denote the shortest path in  $G$  between  $u$  and  $v$  as  $R_{u,v}$ . For a site  $s \in F$  we denote by  $\text{Left}(P, s)$  the set of vertices  $v \in P$  such that  $R_{s,v}$  enters  $P$  from the left.

The following lemma describes a data structure that will later (Lemma 4) allow to find an  $(F, \text{left})$ -partition of  $P$ . A similar proof finds an  $(F, \text{right})$ -partition.

► **Lemma 3** (Enhanced MSSP data structure). *Given a planar graph  $G$ , a face  $f$  and a recursive decomposition  $T$  of  $G$ , one can construct in  $\tilde{O}(n)$  time a data structure supporting the following queries, each in  $\tilde{O}(1)$  time. For any source  $s \in f$ , shortest path  $P \in T$ , and vertex  $v \in P$ :*

1.  $\text{dist}(s, v)$  - return the distance between  $s$  and  $v$  in  $G$ .
2.  $\text{direction}(s, v, P)$  - return whether  $R_{s,v}$  enters  $P$  from left or right.
3.  $\text{count}(s, P, i, j)$  for  $i, j \in P$  - return the number of vertices  $x$  on  $P[i, j] \cap \text{Left}(P, s)$ .
4.  $\text{select}(s, P, i, j, k)$  for  $i, j \in P$  - return the  $k$ 'th vertex  $x$  of  $P[i, j] \cap \text{Left}(P, s)$ .
5.  $\text{ancestor}(s, v, d)$  - return the ancestor of  $v$  that is in depth  $d$  in the shortest paths tree of  $s$ .

The proof of Lemma 3 appears in [2]. In the rest of this section we prove the following.

► **Lemma 4.** *Given  $F$ ,  $H$ , and  $T$ , together with their enhanced MSSP, and a shortest path  $P \in T$ , one can compute an  $(H, \text{left})$ -partition of  $P$ , in  $\tilde{O}(|H|) = \tilde{O}(1)$  time.*

### 3.2 Setup of the query

Recall that the endpoints of  $P$  are  $x$  and  $y$ , and that  $s_x$  and  $s_y$  are the sites of  $H$  such that  $x \in \text{Vor}_H(s_x)$  and  $y \in \text{Vor}_H(s_y)$ . Notice that it is straightforward to find  $s_x$  and  $s_y$  in  $\tilde{O}(|H|) = \tilde{O}(1)$  time by explicitly checking the distance from each of the sites in  $H$  to  $x$  and to  $y$  using the enhanced MSSP. We denote  $R_x = R_{s_x, x}$  and  $R_y = R_{s_y, y}$ . We assume  $s_x \neq s_y$ , since the case  $s_x = s_y$  is a degenerated case.<sup>3</sup> We also assume that  $H \cap P = \emptyset$ , since otherwise we find a partition for  $H \setminus P$ , and then add the intervals of the sites in  $H \cap P$ , using a binary search along  $P$ . The sites  $s_x$  and  $s_y$  partition the face  $F$  into two intervals which we denote by  $F_{\text{left}}$  and  $F_{\text{right}}$ . In addition, let  $H_{\text{left}} = F_{\text{left}} \cap H$  and  $H_{\text{right}} = F_{\text{right}} \cap H$ . The following lemma (see proof in the full version of the paper [2]) states that when computing the  $(H, \text{left})$ -partition, we can ignore every  $s \in H_{\text{right}}$ . Thus, every time we consider a partition with respect to some  $S \subseteq H_{\text{left}}$ , we consider the vertices of  $S$  from the closest vertex to  $s_x$  to the closest vertex to  $s_y$  (on  $F_{\text{left}}$ ). In addition, the partition is always such that the order of the parts corresponding to vertices of  $S$  is from the one containing  $x$  to the one containing  $y$ .

► **Lemma 5.** *Every  $(H_{\text{left}}, \text{left})$ -partition is an  $(H, \text{left})$ -partition.*

<sup>3</sup> If  $s_x = s_y$  one can think of the graph obtained by making an incision along  $R_x$ , which allows us to think of  $s_x$  as being split into two vertices, where one is the site of  $x$  and the other is the site of  $y$ , see also Remark 12.



► **Remark 6.** When considering a partition of  $P$  with respect to a set  $S \subseteq H_{\text{left}}$ , the parts of  $P$  in our partition are chosen so that they are consistent with the order of the vertices in  $S$ . For example, the first part, corresponds to the vertex of  $S$  closest to  $s_x$ , contains  $x$  (unless it is empty) and the part of the vertex closest to  $s_y$ , contains  $y$  (unless it is empty).

**Trimming  $P$ .** By definition  $x \in \text{Vor}_H(s_x)$  and for every  $v \in R_x$  we also have  $v \in \text{Vor}_H(s_x)$ . Therefore, w.l.o.g., we assume that  $R_x \cap P$  contains only the vertex  $x$ , since all the vertices of  $R_x \cap P$  are known to belong to  $\text{Vor}_H(s_x)$ . Similarly, we assume that  $R_y \cap P = \{y\}$ .

**Swirly paths.** For vertices  $s \in F_{\text{left}}$  and  $v \in P$ , we say that  $R_{s,v}$  is a *swirly* path if  $v \in \text{Left}(P, s)$  and  $R_{s,v}$  crosses  $R_x$  or  $R_y$ . Moreover, a path is called *x-swirly* (resp. *y-swirly*) if the first path it crosses among  $R_x$  and  $R_y$  is  $R_x$  (resp.  $R_y$ ).

Swirly paths complicate life. We shall first (in Section 3.3) explain how to obtain an  $(S, \text{left})$ -partition  $P$  when  $|S| = 2$  and there are no swirly paths. We consider the general case (with  $|S| = 2$ ) where there are swirly paths in the full version of the paper [2]. Finally, in Section 3.4 we will show how to obtain an  $(H, \text{left})$ -partition of  $P$ , removing the restriction to two vertices and proving Lemma 4.

### 3.3 Partition with respect to two sites

In this subsection we show how to compute an  $(S, \text{left})$ -partition when  $|S| = 2$ . We start with a special case, where we consider a subpath  $\hat{P}$  of  $P$  that is not involved in any swirly paths. Later, in Lemma 11 we introduce the algorithm for computing an  $(S, \text{left})$ -partition when  $|S| = 2$ .

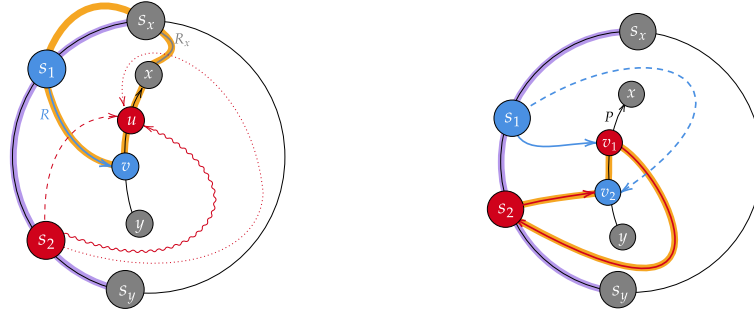
► **Lemma 7.** *Let  $s_1, s_2 \in F_{\text{left}} \setminus P$  be two sites such that  $s_1$  is closer to  $s_x$  on  $F_{\text{left}}$  than  $s_2$ . Let  $\hat{P} = P[a, b]$  be a subpath of  $P$  with  $a$  being closer to  $x$  than  $b$ , such that for every  $i \in \{1, 2\}$  and  $v \in \text{Left}(\hat{P}, s_i)$  the path  $R_{s_i, v}$  is non-swirly. One can compute in  $\tilde{O}(1)$  time an  $(\{s_1, s_2\}, \text{left})$ -partition of  $\hat{P}$  into  $\hat{P}_1, \hat{P}_2$  such that  $a \in \hat{P}_1$  and  $b \in \hat{P}_2$ , unless the partition is trivial.*

The proof of Lemma 7 consists of several steps. We first introduce the notion of *winning*, and show (Claim 8) that it is a monotone property of vertices of  $\hat{P}$ . We will then use this monotonicity to perform binary search. For a vertex  $v \in \hat{P}$  we say that  $s_1$  *wins at  $v$*  if there exists an  $s_1$ -to- $v$  non-swirly path  $R$  that enters  $P$  from the left and  $\text{len}(R) < \text{dist}(s_2, v)$ . We define  $s_2$  *winning at  $v$*  symmetrically.

To avoid clutter we assume  $\hat{P} = P$ , otherwise one just has to change in the following proofs  $P$  to  $\hat{P}$  and  $x, y$  to the endpoints of  $\hat{P}$ .

► **Claim 8.** Let  $v \in P$  such that  $s_1$  wins at  $v$ . Then, every  $u \in P[x, v]$  is a vertex that  $(\{s_1, s_2\}, \text{left})$ -likes  $s_1$ . Symmetrically, if  $s_2$  wins at  $v$ , then every  $u \in P[v, y]$  is a vertex that  $(\{s_1, s_2\}, \text{left})$ -likes  $s_2$ .

**Proof.** We prove the first claim, the proof of the symmetric claim is similar. Since  $s_1$  wins at  $v$ , there exists an  $s_1$ -to- $v$  non-swirly path  $R$  that enters  $P$  from the left and  $\text{len}(R) < \text{dist}(s_2, v)$ . Let  $u \in P[x, v]$ . Assume by contradiction that  $u$  is a vertex that does not  $(\{s_1, s_2\}, \text{left})$ -like  $s_1$ . Then  $R_{s_2, u}$  must enter  $P$  from the left and  $\text{len}(R_{s_2, u}) < \min\{\text{dist}(s_1, u), \text{dist}(s_x, u)\}$ . Hence, for any  $z \in R_{s_2, u}$  we have  $\text{dist}(s_2, z) < \text{dist}(s_1, z)$ . Thus,  $R \cap R_{s_2, u} = \emptyset$ . Similarly, for any  $z \in R_x$  we have  $\text{dist}(s_x, z) < \text{dist}(s_2, z)$ . Hence,  $R_x \cap R_{s_2, u} = \emptyset$ .



■ **Figure 2** Left: The (orange) cycle  $C$  in the proof of Claim 8. The three options for  $R_{s_2,u}$  are in red. Dashed red contradicts  $v$  being closer to  $s_1$  than to  $s_2$ , dotted red contradicts  $x$  being closer to  $s_x$  than to  $s_2$ , and wavy red contradicts  $R_{s_2,u}$  entering  $P$  from the left. Right: The (orange) cycle  $C$  in the proof of Claim 9. Since  $s_1$  is (strictly) on one side of  $C$  and  $v_2$  is on the other side of  $C$ , the dashed  $R_{s_1,v_2}$  path must cross  $C$  in either  $P[v_2, v_1]$  or  $R_{s_2,v_2}$ . Both these crosses are impossible.

Consider the cycle  $C$  composed of  $R, P[v, x]$ ,  $R_x$  and the Jordan curve connecting  $s_x$  and  $s_1$  embedded in the face  $F$ . See Figure 2 (left). Notice that  $C$  has no self-crossing since  $R$  does not cross  $R_x$  as  $R$  is a non-swirly path. We think of  $C$  as an oriented cycle whose orientation is consistent with that of  $P$  (recall that the orientation of  $P$  is from  $y$  to  $x$ ) so as to define left and right properly (i.e., define what is left and right w.r.t.  $C$ ). Observe that  $s_2$  is on the right side of  $C$ . Since  $R_{s_2,u}$  intersects  $C$ , but does not intersect  $R$  nor  $R_x$ , it must be that  $R_{s_2,u}$  intersects only  $P$  among the parts of  $C$ . Since  $s_2$  is on the right side of  $C$ ,  $R_{s_2,u}$  enters  $P$  from the right, a contradiction.  $\triangleleft$

Having proved that the winning property is sufficient to perform a binary search to obtain a partition of  $P$ , we next show how to find a pair  $(s_w, v_t)$  (where  $w \in \{1, 2\}$  and  $t \in \{1, 2\}$ ) such that  $s_w$  is a winner at  $v_t$ . We distinguish two scenarios that are handled differently (Claims 9 and 10). Later we will put it all together and show how to make this into an efficient binary search procedure.

▷ **Claim 9.** Let  $v_1$  and  $v_2$  be vertices such that  $v_1 \in \text{Left}(P, s_1)$  and  $v_2 \in \text{Left}(P, s_2)$ . If  $v_1$  is closer on  $P$  to  $x$  than  $v_2$  then there is an  $\tilde{O}(1)$ -time algorithm that outputs  $w \in \{1, 2\}$  and  $t \in \{1, 2\}$  such that  $s_w$  wins at  $v_t$ .

**Proof.** For every  $w, t$ , we check if  $R_{s_w, v_t}$  enters  $P$  from the left and whether  $\text{dist}(s_w, v_t)$  is smaller than the distance of the other site to  $v_t$ . We return a pair  $w, t$  satisfying the claim. This takes  $\tilde{O}(1)$  time using the enhanced MSSP data structure of Lemma 3.

It remains to prove that at least one such pair exists. Assume by contradiction that no such pair exists. In particular, since  $R_{s_1, v_1}$  enters  $P$  from the left, it must be the case that  $\text{dist}(s_2, v_1) < \text{dist}(s_1, v_1)$ . Moreover,  $R_{s_2, v_1}$  must enter  $P$  from the right (otherwise  $s_2, v_1$  is a valid pair). Similarly, since  $R_{s_2, v_2}$  enters  $P$  from the left we have  $\text{dist}(s_1, v_2) < \text{dist}(s_2, v_2)$ .

We will show that  $R_{s_1, v_2}$  enters  $P$  from the left, implying that  $(s_1, v_2)$  is a valid pair, contradicting our assumption. Consider the (non self crossing) cycle  $C = R_{s_2, v_2} \circ P[v_2, v_1] \circ R_{s_2, v_1}$ . We think of  $C$  as an oriented cycle whose orientation is consistent with that of  $P$  so as to define left and right properly, see Figure 2 (right).

Let  $u$  be the first vertex of  $R_{s_1, v_2}$  that belongs to  $C$ . Note that  $u$  exists since  $v_2 \in C$ . Since  $s_1$  is on the left side of  $C$ ,  $R_{s_1, v_2}$  enters  $C$  from the left at  $u$ . We will show that  $u \notin R_{s_2, v_1}$ , which means that either (i)  $u \in P(v_1, v_2]$  or (ii)  $u \in R_{s_2, v_2}$ . To see that  $u \notin R_{s_2, v_1}$  notice that every  $z \in R_{s_2, v_1}$  satisfies  $\text{dist}(s_2, z) < \text{dist}(s_1, z)$  and every  $z \in R_{s_1, v_2}$  satisfies

$\text{dist}(s_1, z) < \text{dist}(s_2, z)$ . If (i)  $u \in P(v_1, v_2]$  then  $R_{s_2, v_2}$  enters  $P$  from the left, as it enters  $C$  from the left at  $u$ . If (ii)  $u \in R_{s_2, v_2}$  then  $R_{s_1, v_2}[u, v_2] = R_{s_2, v_2}[u, v_2]$ , meaning that  $R_{s_1, v_2}$  enters  $P$  from the left. To conclude, in both cases  $R_{s_1, v_2}$  enters  $P$  from the left, which contradicts our assumption.  $\blacktriangleleft$

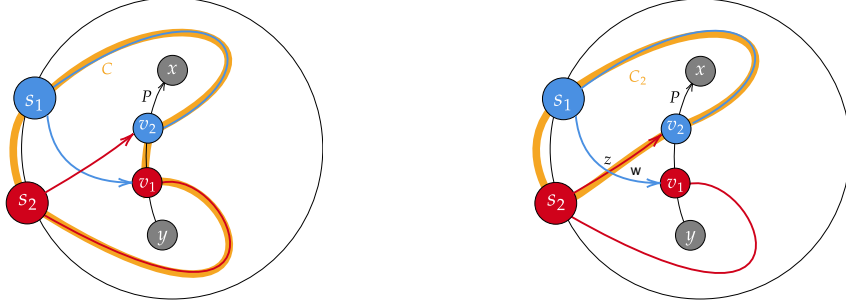


**Figure 3** The (orange) cycles  $C$  (left image) and  $C_2$  (right image) in the proof of Claim 10. The situation here is that  $s_1$  reaches  $v_1$  from the left and loses to  $s_2$  that reaches  $v_1$  from the right, and the symmetric issue for  $v_2$ . Thus,  $v_1$  and  $v_2$  both  $(\{s_1, s_2\}, \text{left})$ -likes both  $s_1$  and  $s_2$ . To recognize a winner we detect which site is closer to  $z$ .

$\triangleright$  **Claim 10.** Let  $v_1$  and  $v_2$  be vertices such that  $v_1 \in \text{Left}(P, s_1)$  and  $v_2 \in \text{Left}(P, s_2)$ . If  $v_2$  is closer on  $P$  to  $x$  than  $v_1$  then there is an  $\tilde{O}(1)$ -time algorithm that outputs  $w \in \{1, 2\}$  and  $t \in \{1, 2\}$  such that  $s_w$  wins at  $v_t$ .

**Proof.** For every  $w, t$  we check if  $R_{s_w, v_t}$  enters  $P$  from the left and whether  $\text{dist}(s_w, v_t)$  is smaller than the distance of the other site to  $v_t$ . If such a pair is found, we return this pair. Otherwise, it must be that: (1)  $\text{dist}(s_2, v_1) < \text{dist}(s_1, v_1)$ , (2)  $R_{s_2, v_1}$  enters  $P$  from the right, (3)  $\text{dist}(s_1, v_2) < \text{dist}(s_2, v_2)$ , and (4)  $R_{s_1, v_2}$  enters  $P$  from the right.

Consider the cycle  $C$  composed of  $R_{s_2, v_1}$ ,  $P[v_1, v_2]$ ,  $R_{s_1, v_2}$ , and the Jordan curve connecting  $s_1$  and  $s_2$  embedded in the face  $F$ . We first claim that all edges entering  $P$  from the left are on the left side of  $C$ . To see this, consider making an incision along  $P$  (duplicating its vertices and edges). Since both  $R_{s_1, v_2}$  and  $R_{s_2, v_1}$  do not cross  $P$  and enter  $P$  from the right, they both use the right copy of  $P$ , and do not intersect the left copy of  $P$ . Hence, the left copy of  $P$ , and hence also all edges entering  $P$  from the left, are on the left side of  $C$ .

The path  $R_{s_1, v_1}$  does not intersect  $R_{s_2, v_1} \setminus P$  (since the former enters  $P$  from the left and the latter enters  $P$  from the right). Moreover, by uniqueness of shortest paths,  $R_{s_1, v_1}$  does not cross  $R_{s_1, v_2}$  nor  $P$ . Thus,  $R_{s_1, v_1}$  does not cross  $C$ . Symmetrically,  $R_{s_2, v_2}$  does not cross  $C$ . Since both  $R_{s_1, v_1}$  and  $R_{s_2, v_2}$  start on  $C$ , do not cross  $C$  and enter  $P$  from the left, they must be on the left side of  $C$ .

Since  $\text{dist}(s_1, v_2) < \text{dist}(s_2, v_2)$ , and  $\text{dist}(s_2, v_1) < \text{dist}(s_1, v_1)$  it must be that  $R_{s_1, v_2} \cap R_{s_2, v_1} = \emptyset$ . Hence, in the counterclockwise cyclic order of  $C$  the vertices appear as  $s_2, v_1, v_2, s_1$ . Therefore, the paths  $R_{s_1, v_1}$  and  $R_{s_2, v_2}$  form a cross configuration and must cross each other, such that  $R_{s_1, v_1}$  crosses  $R_{s_2, v_2}$  from left to right.

For simplicity, we assume that  $R_{s_1, v_1} \cap R_{s_2, v_2}$  contains a single vertex  $z$ . In the general case, it may be a contiguous subpath and the proof is similar. Our goal now is to determine whether  $z$  is closer to  $s_1$  or to  $s_2$ . We emphasize that the algorithm does not find  $z$  itself at any time.

Consider the path  $R_{s_1, v_1}$  and notice that  $\text{dist}(s_1, s_1) < \text{dist}(s_2, s_1)$  and  $\text{dist}(s_2, v_1) < \text{dist}(s_1, v_1)$ . Since  $R_{s_1, v_1}$  is a shortest path, it must be that for some vertex  $w \in R_{s_1, v_1}$  we have that all vertices in  $R_{s_1, v_1}[s_1, w]$  are closer to  $s_1$  than to  $s_2$  and all vertices in  $R_{s_1, v_1}[w, v_1]$  are closer to  $s_2$  than to  $s_1$ . Using  $\text{ancestor}(s_1, v_1, d)$  queries of the enhanced MSSP (in  $\tilde{O}(1)$  time per query), the algorithm binary-searches for  $w$ , checking at every step which of  $s_1$  and  $s_2$  is closer to the queried vertex. After finding  $w$ , the algorithm uses enhanced MSSP to check whether  $w$  appears to the right, to the left, on  $R_{s_2, v_2}$  in the shortest path tree rooted at  $s_2$ . We note that  $w$  cannot be a descendant of  $v_2$  in the tree of  $s_2$ , since every vertex on  $R_{s_2, w}$  is closer to  $s_2$  than to  $s_1$ , while  $v_2$  is closer to  $s_1$  than to  $s_2$ . If  $w$  is on  $R_{s_2, v_2}$  then  $z = w$  is closer to  $s_2$  than to  $s_1$ .

We will show that if  $w$  is to the right of  $R_{s_2, v_2}$  in the tree of  $s_2$  then  $z$  is closer to  $s_1$  than to  $s_2$ . Consider the cycle  $C_2$  obtained by concatenating  $R_{s_2, v_2}, R_{v_2, s_1}$  and the Jordan curve connecting  $s_1$  and  $s_2$  embedded in the face  $F$ . We consider  $C_2$  to be oriented from  $s_2$  to  $v_2$ . Notice that  $R_{s_1, v_1}[s_1, z]$  does not cross  $C_2$  since  $R_{s_1, v_1}$  and  $R_{s_2, v_2}$  cross each other only once. Recall that  $R_{s_1, v_1}[s_1, z]$  is to the left of  $R_{s_2, v_2}$ , and therefore to the left of  $C_2$ . Additionally recall  $R_{s_1, v_1}[z, v_1]$  is to the right of  $R_{s_2, v_2}$ , and therefore to the right of  $C_2$ . Consider the first vertex  $u$  of  $R_{s_2, w}$  which is not on  $R_{s_2, v_2}$ . Since  $w$  is to the right of  $R_{s_2, v_2}$ , it holds that  $u$  is to the right of  $C_2$ . Moreover  $Q = R_{s_2, w}[u, w]$  is strictly to the right of  $C_2$ . This is because  $Q$  is disjoint from  $R_{s_2, v_2}$  by uniqueness of shortest paths, and is disjoint from  $R_{s_1, v_2}$  since  $v_2$  is closer to  $s_1$  and  $w$  is closer to  $s_2$ . Thus,  $Q$  is disjoint from  $C_2$ , and therefore  $w$  is to the right of  $C_2$  and therefore  $w \in R_{s_1, v_1}(z, v_1]$  and this means  $z$  is closer to  $s_1$  than to  $s_2$  by definition of  $w$ . A similar argument shows that if  $w$  is to the left of  $R_{s_2, v_2}$  in the shortest paths tree of  $s_2$ , then  $z$  is closer to  $s_2$  than to  $s_1$ .

Thus, the algorithm deduces whether  $z$  is closer to  $s_1$  or to  $s_2$ . If  $z$  is closer to  $s_1$ , the algorithm reports that  $s_1$  wins at  $v_2$ . This is because the path  $R = R_{s_1, v_1}[s_1, z] \circ R_{s_2, v_2}[z, v_2]$  enters  $P$  from the left and  $\text{len}(R) < \text{dist}(s_2, v_2)$ . Moreover,  $R$  is a concatenation of subpaths of two non-swirly paths from vertices on  $F_{\text{left}}$ , and therefore  $R$  is a non-swirly path. Similarly, if  $z$  is closer to  $s_2$ , the algorithm reports that  $s_2$  wins at  $v_1$ . This is because the path  $R = R_{s_2, v_2}[s_2, z] \circ R_{s_1, v_1}[z, v_1]$  enters  $P$  from the left and  $\text{len}(R) < \text{dist}(s_1, v_1)$ , and  $R$  is a non-swirly path.

Finally, the running time of the algorithm is indeed  $\tilde{O}(1)$ , since all distance queries, and directions can be answered in  $\tilde{O}(1)$  time per query by the enhanced MSSP of Lemma 3 and the binary search of  $w$  increases the running time only by an additional  $\tilde{O}(1)$  factor.  $\triangleleft$

Using Claims 8–10 we introduce a recursive binary search partition algorithm, completing the proof of Lemma 7. In each recursive step, the algorithm works on a subpath  $\bar{P} = P[a, b]$ , and returns a partition of  $\bar{P}$  into a (possibly empty) prefix  $\bar{P}_1$  and a (possibly empty) suffix  $\bar{P}_2$  such that every  $v \in \bar{P}_i$  is a vertex that  $(\{s_1, s_2\}, \text{left})$ -likes  $s_i$  (for  $i \in \{1, 2\}$ ).

When working on  $\bar{P} = P[a, b]$ , the algorithm starts by finding a “left median” vertex of  $s_1$  in  $P[a, b]$ . Formally, a left median of  $s_1$  in  $P[a, b]$  is a vertex  $v_1 \in P[a, b]$  such that the shortest path between  $s_1$  and  $v_1$  enters  $P$  from the left, and the number of vertices whose shortest path from  $s_1$  enters  $P$  from the left in  $P[a, v_1]$  differs by at most 1 from the number of vertices whose shortest path from  $s_1$  enters  $P$  from the left in  $P[v_1, b]$ . The algorithm finds left medians  $v_1$  and  $v_2$  for  $s_1$  and  $s_2$ , respectively, in  $P[a, b]$  by using a count query to the enhanced MSSP, and then applying binary search using select and count queries.

If no left-median exists for  $s_1$ , the algorithm returns the partition  $\bar{P}_1 = \emptyset$  and  $\bar{P}_2 = \bar{P} = P[a, b]$ . Similarly, if no left-median exists for  $s_2$ , the algorithm returns the partition  $\bar{P}_1 = \bar{P}$  and  $\bar{P}_2 = \emptyset$ . Otherwise, depending on the order of  $v_1$  and  $v_2$  on  $P$ , the algorithm either applies Claim 9 or Claim 10 to find  $w \in \{1, 2\}$  and  $t \in \{1, 2\}$  such that  $s_w$  wins at

$v_t$ . If  $w = 1$ , the algorithm recursively obtains a partition  $(P'_1, P'_2)$  of  $P(v_t, b]$ , and returns  $\bar{P}_1 = P[a, v_t] \circ P'_1$  and  $\bar{P}_2 = P'_2$ . If  $w = 2$ , the algorithm recursively obtains a partition  $(P'_1, P'_2)$  of  $P[a, v_t)$  and returns  $\bar{P}_1 = P'_1$  and  $\bar{P}_2 = P'_2 \circ P[v_t, b]$ .

**Correctness.** The correctness of the halting condition follows from the definition of an  $(\{s_1, s_2\}, \text{left})$ -partition. If there is no left-median for  $s_1$  (resp.  $s_2$ ), in particular there are no vertices that  $s_1$  (resp.  $s_2$ ) reaches from the left on  $\bar{P}$ . Therefore, every vertex on  $\bar{P}$  is a vertex that  $(\{s_1, s_2\}, \text{left})$ -likes  $s_2$  (resp.  $s_1$ ) and therefore a partition that sets  $P_2 = \bar{P}$  (resp.  $P_1 = \bar{P}$ ) is valid. The correctness of the recursive step of the algorithm follows directly from Claim 8 and the correctness of the recursion.

**Complexity.** The non-recursive part of the algorithm consists of a polylogarithmic number of queries for the enhanced MSSP, and therefore takes  $\tilde{O}(1)$  time. We claim that the recursion depth is bounded by  $O(\log n)$ . This is because in every recursive step the algorithm either reduces the number of vertices that  $s_1$  reaches from the left or the number of vertices that  $s_2$  reaches from the left - by half. Since initially each of these numbers is bounded by  $|P| \leq n$ , a halting condition must be satisfied after at most  $2 \log n$  recursive calls. The overall time complexity is therefore  $\tilde{O}(1)$  thus completing the proof of Lemma 7. ◀

The following Lemma is the general version of Lemma 7 in the presence of swirly paths.

► **Lemma 11** (See proof in the full version [2]). *Let  $s_1, s_2 \in F_{\text{left}} \setminus P$  be two sites such that  $s_1$  is closer to  $s_x$  on  $F_{\text{left}}$  than  $s_2$ . One can compute in  $\tilde{O}(1)$  time an  $(\{s_1, s_2\}, \text{left})$ -partition of  $P$  into  $P_1, P_2$  such that  $x \in P_1$  and  $y \in P_2$ , unless the partition is trivial.*

### 3.4 Relaxed partition for $H$ (proof of Lemma 4)

Using Lemma 11 we are finally ready to prove Lemma 4 on the construction of a relaxed partition for  $H$ . By Lemma 5, it is enough to compute an  $(H_{\text{left}}, \text{left})$ -partition. If  $|H_{\text{left}}| = 1$  the partition is trivial. If  $|H_{\text{left}}| = 2$  we obtain the partition from Lemma 11. When  $|H_{\text{left}}| = 3$  with  $s_1, s_2, s_3$  being the three sites according to their order on  $F_{\text{left}}$ , starting from  $s_1 = s_x$ , we apply Lemma 11 on three pairs  $(s_1, s_2)$ ,  $(s_2, s_3)$  and  $(s_1, s_3)$ . Let  $P_i^{j,k}$  denote that part corresponds to  $s_i$  in the partition computed for  $(s_j, s_k)$ . If  $P_2^{1,2} \cap P_2^{2,3} \neq \emptyset$  the algorithm returns  $P_1^{1,2}, P_2^{1,2} \cap P_2^{2,3}, P_2^{2,3}$ . Otherwise, if  $P_2^{1,2} \cap P_2^{2,3} = \emptyset$  the algorithm returns  $P_1^{1,3}, P_3^{1,3}$ . Clearly, the algorithm takes  $\tilde{O}(1)$  time.

**Correctness.** We first consider the case where  $P_2^{1,2} \cap P_2^{2,3} = \emptyset$ . Let  $v \in P_1^{1,3}$  and assume to the contrary that  $v$  does not  $(\{s_1, s_2, s_3\}, \text{left})$ -like  $s_1$ . It must be that there exists  $c \in \{s_1, s_2, s_3, s_x, s_y\}$  such that  $v \in \text{Vor}_{\{s_1, s_2, s_3, s_x, s_y\}}(c)$  and  $v \in \text{Left}(P, c)$ . Since  $v$  is a vertex that  $(\{s_1, s_3\}, \text{left})$ -likes  $s_1$ , it must be that  $c = s_2$ . However, this means that  $v$  does not  $(\{s_1, s_2\}, \text{left})$ -like  $s_1$  and also  $v$  does not  $(\{s_2, s_3\}, \text{left})$ -like  $s_3$ . Hence,  $v \in P_2^{1,2} \cap P_2^{2,3}$ , a contradiction. Thus,  $v$  indeed  $(\{s_1, s_2, s_3\}, \text{left})$ -likes  $s_1$ . The proof for vertices in  $P_3^{1,3}$  is similar.

We next consider the case  $P_2^{1,2} \cap P_2^{2,3} \neq \emptyset$ . For this case we first prove that every  $v \in P_2 = P_2^{1,2} \cap P_2^{2,3}$  must  $(\{s_1, s_2, s_3\}, \text{left})$ -like  $s_2$ . Assume to the contrary that there exists some  $v \in P_2$  such that  $v \in \text{Vor}_{\{s_1, s_2, s_3, s_x, s_y\}}(c)$  and  $v \in \text{Left}(P, c)$  and  $c \in \{s_1, s_2, s_3\}$  and  $c \neq s_2$ . W.l.o.g. we can assume  $c = s_1$  (the case  $c = s_3$  is symmetric). However, in this case  $v$  does not  $(\{s_1, s_2\}, \text{left})$ -like  $s_2$ , contradicting  $v \in P_2^{1,2}$ .

### 33:14 Faster Construction of a Planar Distance Oracle with $\tilde{O}(1)$ Query Time

Finally, we prove that every  $v \in P_1^{1,2}$  must be  $(\{s_1, s_2, s_3\}, \text{left})$ -like  $s_1$  (the proof for  $P_3^{2,3}$  is symmetric). Notice that  $P_1^{1,2} \subset P_2^{2,3}$  since  $P_2^{1,2} \cap P_2^{2,3} \neq \emptyset$ . Assume to the contrary there exists some  $v \in P_1^{1,2}$  such that  $v \in \text{Vor}_{\{s_1, s_2, s_3, s_x, s_y\}}(c)$  and  $v \in \text{Left}(P, c)$  and  $c \in \{s_1, s_2, s_3\}$  and  $c \neq s_1$ . It cannot be that  $c = s_2$ , because  $v \in P_1^{1,2}$ . Assume  $c = s_3$ , then we have that  $v$  does not belong to  $(\{s_2, s_3\}, \text{left})$ -like  $s_2$ , contradicting  $v \in P_1^{1,2} \subset P_2^{2,3}$ .

**Complexity.** Finally, the running time of the algorithm is  $\tilde{O}(1)$  since all distance and direction queries are answered in  $\tilde{O}(1)$  time per query by the enhanced MSSP data structure of Lemma 3 and the binary search of  $w$  increases the running time only by additional  $\tilde{O}(1)$  time. This concludes the proof of Lemma 4.

► **Remark 12.** We note that the proof of Lemma 4 is written for  $|H| = 3$ . However, the algorithm described in the proof can be easily generalized to an algorithm that constructs a partition for a set of  $k$  sites from a partition of  $k - 1$  sites. A standard amortization argument shows that the total running time for constructing a partition of  $k$  sites is  $\tilde{O}(k)$ .

## 4 From a Relaxed Partition to a Trichromatic Face

In this section we prove that one can find a trichromatic face in  $\tilde{O}(1)$  time.

► **Lemma 13.** *Given a planar graph  $G$ , and a face  $F$ , one can preprocess  $G$  in  $\tilde{O}(|G|)$  time such that given a subset  $H \subseteq F$  of 3 sites, and additive weights  $w : H \rightarrow \mathbb{R}^+$ , one can compute the trichromatic face of  $\text{VD}(H, w)$  in time  $\tilde{O}(1)$ .*

**Proof.** Recall that a trichromatic VD (a VD with three sites) has at most one trichromatic face  $\hat{f}$  (apart from the face containing the three sites). We show how to identify  $\hat{f}$  recursively, starting from the root  $G$  of the recursive decomposition tree  $T$ . At a step of the recursion involving a subgraph  $X$ , we determine whether  $\hat{f}$  is enclosed by the cycle separator  $Q$  of  $X$  or not, and recurse on the appropriate child of  $X$  in  $T$  until we get to a subgraph of constant size that contains  $\hat{f}$  (in which we identify  $\hat{f}$  trivially using  $O(1)$  distance queries from the sites using the MSSP data structure in  $O(\log n)$  time).

We obtain a relaxed partition of  $Q$  using Lemma 4. We next explain how to use the relaxed partition to deduce whether  $\hat{f}$  is enclosed by  $Q$  or not. The following immediate consequence of the Jordan curve theorem implies that it suffices to compute the parity of the number of crossings of the three bisectors forming the trichromatic VD. The challenge is that each bisector may cross  $Q$  many times (even  $\Theta(n)$  times), so we cannot afford to actually count all of the crossings in order to compute the parity.

► **Claim 14.** The trichromatic face  $\hat{f}$  is enclosed by  $Q$  if and only if each of the 3 bisectors that meet at  $\hat{f}$  crosses  $Q$  an odd number of times.

**Proof.** In the trichromatic VD, each of the three bisectors originates at the face  $F$  and terminates at  $\hat{f}$ . The cycle separator  $Q$  partitions the faces of  $G$  into two sets, and by definition of  $F$  as the infinite face, and of enclosure,  $F$  is not enclosed by  $Q$ . By the Jordan Curve theorem, any path in the plane starts at a point not enclosed by  $Q$  and ends at a point enclosed by  $Q$  if and only if it crosses  $Q$  an odd number of times. ◀

The relaxed partition of  $Q$  consists of  $O(1)$  intervals for each of the two paths forming  $Q$ , and each of the two sides of these paths. The  $O(1)$  endpoints of all these intervals partition  $Q$  into  $O(1)$  intervals. Consider such an interval  $I$  of  $Q$ . The vertices of  $I$  are all assigned by the relaxed partition a single site from each side. Hence, the vertices of  $I$  belong to at



most two Voronoi cells in  $VD$ . Therefore, the interval  $I$  can only be crossed by the bisector between these two cells. Moreover, the bisector crosses  $I$  an even number of times if and only if both endpoints of  $I$  belong to the same cell. We can determine whether this is the case or not by using  $O(1)$  MSSP queries on the endpoints of  $I$ .

Thus, we can determine the parity of the number of crossings of  $Q$  by each bisector by summing the parities contributed by each of the  $O(1)$  intervals, and deduce if  $\hat{f}$  is enclosed by  $Q$  in  $O(\log n)$  time.  $\blacktriangleleft$

## 5 Computing the Voronoi Diagram

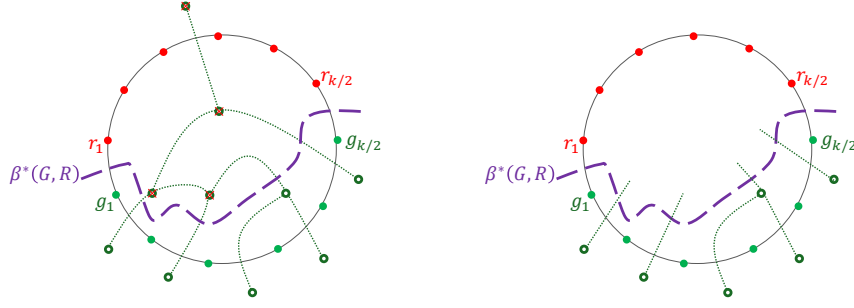
In this section, we describe an algorithm that, given access to the mechanism for computing trichromatic faces provided by Lemma 13, computes  $VD^*(F)$  in  $\tilde{O}(|F|)$  time. Thus, we establish the main theorem of this paper (note that we use  $F$  to denote both the set of sites and the face to which they belong):

► **Theorem 15.** *Given a planar graph  $X$ , and a face  $F$ , one can preprocess  $X$  in  $\tilde{O}(|X|)$  time such that given additive weights  $\omega : F \rightarrow \mathbb{R}^+$ , one can compute  $VD^*(F)$  in  $\tilde{O}(|F|)$  time.*

**Representing the Diagram.** We use the definitions of the dual Voronoi diagram  $VD^*(F)$  from [9]. As was done there, we assume that the graph we work with is triangulated, except for the single face  $F$ , whose vertices are exactly the set of sites of the diagram. We also assume that each site induces a non empty Voronoi cell (including at least the site itself). Thus,  $VD^*(F)$  is a degree-3 tree with  $O(|F|)$  nodes whose leaves are the copies of the dual vertex  $F^*$  (corresponding to the face  $F$ ). Following [20], we use the Doubly-Connected Edge List (DCEL) data structure for representing planar maps to represent the tree  $VD^*(F)$ .

**The Divide-and-Conquer Mechanism.** Denote  $|F| = k$ . We describe a divide-and-conquer algorithm for constructing  $VD^*(F)$  in  $\tilde{O}(k)$  time. If  $k < 3$  then  $VD^*(F)$  contains no trichromatic vertices and its representation is trivial. If  $k = 3$ , then  $VD^*(F)$  consists of either no trichromatic faces or just the single trichromatic face  $\hat{f}$  obtained using Section 4. When  $k > 3$  we partition the set  $S$  of sites into two contiguous subsets along the face  $F$  of (roughly)  $k/2$  sites each. For simplicity, we assume that each subset has size exactly  $k/2$ . We call the sites  $G = g_1, \dots, g_{k/2}$  in one subset the green sites, listed in counterclockwise order along  $F$ . Similarly, we call the other subset  $R = r_1, \dots, r_{k/2}$  the red sites, listed in clockwise order along  $F$ . Note that the ordering is such that  $g_1$  and  $r_1$  are neighboring sites on the face  $F$ . We recursively compute  $VD^*(G)$  and  $VD^*(R)$ , the Voronoi diagram of  $G$  and of  $R$ , respectively. We now describe how to merge these two diagrams into  $VD^*(F)$  in  $\tilde{O}(k)$  time. The idea is similar to the stitching algorithm used in [20]. The main differences are that unlike [20] we have not precomputed the bisectors, but on the other hand, we utilize the point location mechanism of  $VD^*(G)$  and  $VD^*(R)$ , which was not done in [20]. In a nutshell, consider a super green vertex  $G$  connected to all green sites with edges whose lengths correspond to the additive weight to each green site. Similarly, consider a super red vertex  $R$ . Now consider the bisector  $\beta^*(G, R)$ .  $VD^*(F)$  is obtained by cutting both  $VD^*(G)$  and  $VD^*(R)$  along  $\beta^*(G, R)$ , “glueing” the green side (according to  $\beta^*(G, R)$ ) of  $VD^*(G)$  with the red side of  $VD^*(R)$ .

This intuitive process can be performed efficiently using the following procedure. To cut  $VD^*(G)$  along  $\beta^*(G, R)$ , we go over the  $O(k/2)$  nodes of  $VD^*(G)$ . Each of these nodes corresponds to a trichromatic face  $f$  (or to an edge of the hole  $F$  if the node is a leaf of  $VD^*(G)$ ). For each vertex  $v$  of  $f$  (there are 3 or 2 such vertices depending on whether we



■ **Figure 4** A schematic demonstration of the Voronoi vertex deletion process caused by the interaction of the  $\beta^*(G, R)$  bisector with the green diagram  $\text{VD}^*(G)$ . Left: the  $\text{VD}^*(G)$  diagram of the green sites, represented in dotted green lines, and the bisector  $\beta^*(G, R)$  represented in a dashed purple line. The Voronoi (dual) vertices are represented in hollow green circles. The Vertices deleted in the process are crossed in red. Right: the remaining connected components and their respective dangling Voronoi edges after the deletion process.

handle an internal node or a leaf of  $\text{VD}^*(G)$ ), let  $g_i$  be the green site closest (in the sense of additive distance) to  $v$  (the identity of  $g_i$  is stored explicitly in the representation of  $\text{VD}^*(G)$ ). We perform a point location query for  $v$  in  $\text{VD}^*(R)$ , obtaining the red site  $r_j$  closest (in the sense of additive distance) to  $v$ . We compare the distance from  $r_j$  to  $v$  with the distance from  $g_i$  to  $v$  (these distances are available through the MSSP data structure for  $F$ ). If the distance from  $r_j$  is smaller, we know that  $f$  is not a trichromatic face in  $\text{VD}^*(F)$ , so we delete the corresponding node from  $\text{VD}^*(G)$ .<sup>4</sup>

Some Voronoi edges of  $\text{VD}^*(G)$  have both their endpoints deleted by this process. These edges are entirely on the red side of  $\beta^*(G, R)$ , and do not participate in  $\text{VD}^*(F)$ . Other edges have both their endpoints not deleted. These edges are entirely on the green side of  $\beta^*(G, R)$ , and are part of  $\text{VD}^*(F)$ . We call the Voronoi edges with one endpoint deleted and the other not deleted *dangling* edges. The bisector  $\beta^*(G, R)$  intersects  $\text{VD}^*(G)$  at the dangling edges. We associate each dangling edge with the two green sites whose Voronoi cells are on either side of the dangling edge. We prove that there is at most a single dangling edge in each of the components of  $\text{VD}^*(G)$  obtained by the above deletion process.

► **Lemma 16.** *When the deletion process described above terminates, each surviving connected component of  $\text{VD}^*(G)$  contains at most a single dangling edge.*

**Proof.** Assume towards contradiction that some connected component of  $\text{VD}^*(G)$  contains two edges  $e_1, e_2$  crossed by  $\beta^*(G, R)$ . Note that none of the endpoints of  $e_1$  and  $e_2$  that were not deleted by the process is a leaf (or else the connected component would consist of just that leaf). Let  $f_1$  (resp.,  $f_2$ ) be the dual vertex (primal face) in the intersection of the bisector corresponding to  $e_1$  (resp.,  $e_2$ ) and  $\beta^*(G, R)$ . Consider the cycle  $C$  formed by the unique path in  $\text{VD}^*(G)$  between  $f_1$  and  $f_2$ , and the portion of  $\beta^*(G, R)$  between  $f_1$  and  $f_2$ . See Figure 5 (left) for an illustration. Observe that the cycle  $C$  encloses no green sites because the path in  $\text{VD}^*(G)$  between  $f_1$  and  $f_2$  contains no leaves of  $\text{VD}^*(G)$ , so it is disjoint from  $F$ , and because the bisector  $\beta^*(G, R)$  is disjoint from  $F$  except for its first and last edge by our assumption that the sites are contiguous along  $F$  and that every site is in its own Voronoi cell. A contradiction now arises because the cycle  $C$  encloses some primal vertex

<sup>4</sup> To be precise,  $f$  might be a trichromatic face of  $\text{VD}^*(F)$ , but it is not an all-green trichromatic face in  $\text{VD}^*(F)$ , so it is not contributed to  $\text{VD}^*(F)$  by  $\text{VD}^*(G)$ .

$v$  that belongs to a Voronoi cell of some green site  $g_i$ , but the shortest path from  $g_i$  to  $v$  cannot cross into  $C$ ; It cannot cross any bisector of  $\text{VD}^*(G)$  because one endpoint of such a crossing edge does not belong to the cell of  $g_i$  in  $\text{VD}^*(G)$ . It cannot cross  $\beta^*(G, R)$  because one endpoint of such a crossing edge does not belong to the green cell of  $\text{VD}^*(\{G, R\})$ .  $\blacktriangleleft$

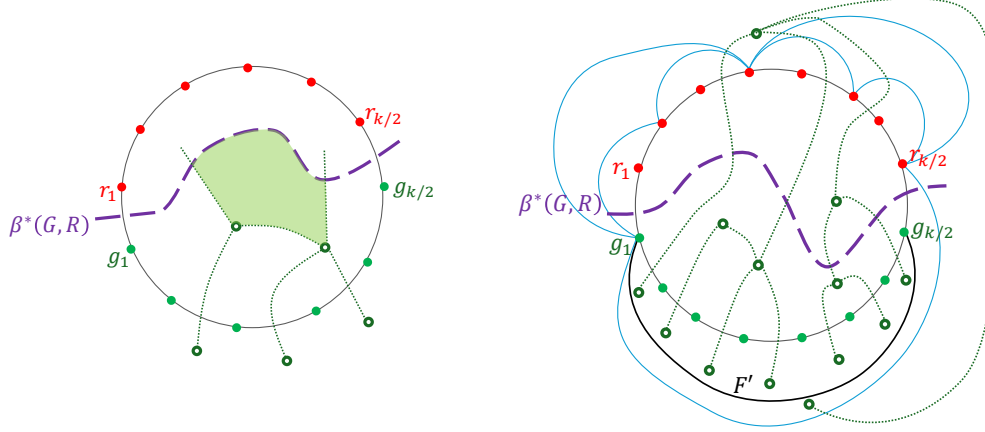


**Figure 5** Left: The cycle  $C$  (enclosing the shaded green area) for the contradiction in the proof of Lemma 16. Right: Enforcing the assumptions before the recursive call that computes  $\text{VD}^*(G)$ . The bold black edge guarantees that the green sites are exactly the sites of a face (the face  $F'$ ). The blue artificial edges guarantee triangulation.

Having found the components of  $\text{VD}^*(G)$  (and by a similar process of  $\text{VD}^*(R)$ ) that form  $\text{VD}^*(F)$ , we trace  $\beta^*(G, R)$ , and stitch the components of  $\text{VD}^*(G)$  and  $\text{VD}^*(R)$  at new trichromatic vertices that we identify along the way. The first endpoint of  $\beta^*(G, R)$  (which is a leaf of  $\text{VD}^*(F)$ ) is a copy of  $F^*$  that lies at the end of a dual of the edge of  $F$  separating between the sites  $g_i = g_1$  and  $r_j = r_1$ . The next trichromatic vertex along  $\beta^*(G, R)$  occurs when  $\beta^*(G, R)$  intersects the boundary of the Voronoi cell of either  $g_i$  or of  $r_j$ .

Recall that each dangling edge with the two green sites whose Voronoi cells are on either side of the dangling edge. We shall prove in Lemma 17, that the sites  $g_1$  and  $g_{k/2}$  are associated with exactly one dangling edge, and all other sites are associated with either two or zero dangling edges. To identify the next trichromatic vertex of  $\text{VD}^*(F)$  along  $\beta^*(G, R)$ , we inspect the dangling edge associated with  $g_i$ . When  $g_i = g_1$ , there is only one associated dangling edge. In general, there are two associated dangling edges, but only one was not yet handled by the stitching process. The dangling edge that was not yet handled represents a bisector between two green sites. One of them must be  $g_i$  (since the intersection is a trichromatic face on the boundary of the Voronoi cell of  $g_i$ ). Denote the other one by  $g_{i'}$ . Similarly, a possible candidate for the next trichromatic vertex of  $\text{VD}^*(F)$  along  $\beta^*(G, R)$  may come from the yet unhandled dangling edge of a connected component of  $\text{VD}^*(R)$  that is associated with  $r_j$ , which represents a bisector between  $r_j$  and some other red site  $r_{j'}$ .

We use Lemma 13 to find the two possible candidates: the trichromatic face  $f_g$  of  $(r_j, g_i, g_{i'})$  and the trichromatic face  $f_r$  of  $(r_j, r_{j'}, g_i)$ . Only one of them is a true trichromatic vertex of  $\text{VD}^*(F)$ , which can be decided by using the same point location process we had used in the deletion process for each of its incident primal vertices. Suppose w.l.o.g. that we identified that the next trichromatic face is the face  $f_g$  of  $(r_j, g_i, g_{i'})$  (the procedure for  $f_r$  is symmetric). We connect in  $\text{VD}^*(S)$  the previous trichromatic face on  $\beta^*(G, R)$  with  $f_g$  via a new Voronoi edge, and make  $f_g$  the new endpoint of the dangling edge associated with  $g_i$ .

Next, we infer the identity of the edge of the  $\beta^*(G, R)$  bisector leaving  $f_g$  via which the traversal of  $\beta^*(G, R)$  continues. Since  $f_g$  was the new trichromatic face, then  $\beta^*(G, R)$  just crossed in  $\text{VD}^*(G)$  from the cell of  $g_i$  to the cell of  $g_{i'}$ , so we repeat the process of finding the next trichromatic face along  $\beta^*(G, R)$  with sites  $r_j$  and  $g'_i$ . The process terminates when it has handled all of the dangling edges in all the components of  $\text{VD}^*(G)$  and  $\text{VD}^*(R)$ .

To complete the correctness argument it remains to prove the bound on the association between sites and dangling edges (Lemma 17). However, before doing that, we need to elaborate on a technical issue we had glossed over in the description of the recursive approach. We had assumed that in any  $\text{VD}^*$  in the recursion, the sites are exactly the vertices of some face  $F$  of the graph  $X$  in which  $\text{VD}^*$  is computed, and that  $F$  is the only face of  $X$  that is not a triangle. To satisfy this requirement, before making the recursive call that computes  $\text{VD}^*(G)$ , we add to  $X$  an artificial infinite-length edge connecting  $g_1$  and  $g_{k/2}$ . This artificial edge is embedded in the face  $F$ , splitting it into two new faces  $F'$  and  $F''$ , such that the vertices of  $F'$  are exactly the green sites. We triangulate  $F''$  with infinite length edges. Let  $X'$  denote the resulting graph. See Figure 5 (right). Note that  $X'$  now satisfies the assumptions so we can invoke the construction algorithm recursively on  $X'$  and obtain  $\text{VD}^*(G)$ . In  $\text{VD}^*(G)$ , the boundary of the Voronoi cell of each  $g_i$  forms a simple path between the two leaves (copies of  $F'$  corresponding to dual edges of  $F'$  between  $g_{i-1}g_i$  and  $g_i g_{i+1}$ ) in  $\text{VD}^*(G)$ , which we associate with  $g_i$ . Note that for sites  $g_i$  for  $1 < i < k/2$ , both associated leaves are real edges of  $P$ , whereas for  $g_1$  and  $g_{k/2}$  one leaf is real, but the other is dual to an artificial edge of  $X'$ .

Since  $\text{VD}^*(G)$  may contain (dual) artificial vertices (i.e., faces  $X'$  that are not faces of  $X$ ), at the beginning of the deletion process we delete all artificial vertices of  $\text{VD}^*(G)$ , and then apply the deletion process described above. Observe that exactly one of the leaves corresponding to  $g_1$  and  $g_{k/2}$  is deleted by the deletion process, and none of the two leaves associated with the other sites is deleted. This is because each  $G_i$  is in its own Voronoi cell in  $\text{VD}^*(F)$ .

► **Lemma 17.** *When the deletion process of  $\text{VD}^*(G)$  described above terminates, sites  $g_1$  and  $g_{k/2}$  are associated with exactly one dangling edge, and all other sites are associated with either two or zero dangling edges.*

**Proof.** The deletion process deletes a single contiguous subpath from the boundary of each Voronoi cell. This is because otherwise, there would be a resulting connected component that contains two dangling edges, contradicting Lemma 16. Thus, since the dangling edges associated with site  $g_i$  are the dangling edges on the boundary of the Voronoi cell of  $g_i$ , each site is associated with at most two dangling edges. Since for  $g_1$  and  $g_{k/2}$  exactly one of the corresponding leaves are deleted, the process results in a single dangling edge associated with each of these two sites. For all other sites, none of the two corresponding leaves are deleted, hence there are two associated dangling edges with each site other than  $g_1$  and  $g_{k/2}$ . ◀

---

## References

- 1 Srinivasa Rao Arikati, Danny Z. Chen, L. Paul Chew, Gautam Das, Michiel H. M. Smid, and Christos D. Zaroliagis. Planar spanners and approximate shortest path queries among obstacles in the plane. In *Proceedings 4th Annual European Symposium on Algorithms (ESA)*, volume 1136, pages 514–528, 1996. doi:10.1007/3-540-61680-2\_79.
- 2 Itai Boneh, Shay Golan, Shay Mozes, Daniel Prigan, and Oren Weimann. Faster construction of a planar distance oracle with  $\tilde{o}(1)$  query time. *CoRR*, abs/2503.18425, 2025. doi:10.48550/arXiv.2503.18425.

- 3 Glencora Borradaile, Piotr Sankowski, and Christian Wulff-Nilsen. Min *st*-cut oracle for planar graphs with near-linear preprocessing time. *ACM Transactions on Algorithms*, 11(3):1–29, 2015. doi:10.1145/2684068.
- 4 Sergio Cabello. Many distances in planar graphs. *Algorithmica*, 62(1-2):361–381, 2012. doi:10.1007/s00453-010-9459-0.
- 5 Sergio Cabello. Subquadratic algorithms for the diameter and the sum of pairwise distances in planar graphs. *ACM Trans. Algorithms*, 15(2):21:1–21:38, 2019. doi:10.1145/3218821.
- 6 Sergio Cabello, Erin W. Chambers, and Jeff Erickson. Multiple-source shortest paths in embedded graphs. *SIAM J. Comput.*, 42(4):1542–1571, 2013. doi:10.1137/120864271.
- 7 Parinya Chalermsook, Jittat Fakcharoenphol, and Danupon Nanongkai. A deterministic near-linear time algorithm for finding minimum cuts in planar graphs. In J. Ian Munro, editor, *Proceedings of the Fifteenth Annual ACM-SIAM Symposium on Discrete Algorithms, SODA 2004, New Orleans, Louisiana, USA, January 11-14, 2004*, pages 828–829. SIAM, 2004. URL: <http://dl.acm.org/citation.cfm?id=982792.982916>.
- 8 Timothy M. Chan and Dimitrios Skrepetos. Faster approximate diameter and distance oracles in planar graphs. *Algorithmica*, 81(8):3075–3098, 2019. doi:10.1007/s00453-019-00570-z.
- 9 Panagiotis Charalampopoulos, Paweł Gawrychowski, Yaowei Long, Shay Mozes, Seth Pettie, Oren Weimann, and Christian Wulff-Nilsen. Almost optimal exact distance oracles for planar graphs. *J. ACM*, 70(2):12:1–12:50, 2023. doi:10.1145/3580474.
- 10 Panagiotis Charalampopoulos, Paweł Gawrychowski, Shay Mozes, and Oren Weimann. Almost optimal distance oracles for planar graphs. In *Proceedings of the 51st Annual ACM Symposium on Theory of Computing (STOC)*, pages 138–151, 2019.
- 11 Panagiotis Charalampopoulos, Paweł Gawrychowski, Shay Mozes, and Oren Weimann. An almost optimal edit distance oracle. In *Proceedings of the 48th International Colloquium on Automata, Languages, and Programming, (ICALP)*, volume 198, pages 48:1–48:20, 2021. doi:10.4230/LIPICS.ICALP.2021.48.
- 12 Panagiotis Charalampopoulos and Adam Karczmarz. Single-source shortest paths and strong connectivity in dynamic planar graphs. *J. Comput. Syst. Sci.*, 124:97–111, 2022. doi:10.1016/J.JCSS.2021.09.008.
- 13 Danny Z. Chen and Jinhui Xu. Shortest path queries in planar graphs. In *Proceedings of the 32nd Annual ACM Symposium on Theory of Computing (STOC)*, pages 469–478, 2000. doi:10.1145/335305.335359.
- 14 Vincent Cohen-Addad, Søren Dahlgaard, and Christian Wulff-Nilsen. Fast and compact exact distance oracle for planar graphs. In *Proceedings 58th Annual IEEE Symposium on Foundations of Computer Science (FOCS)*, pages 962–973, 2017. doi:10.1109/FOCS.2017.93.
- 15 Hristo Djidjev. Efficient algorithms for shortest path queries in planar digraphs. In *Proceedings of the 22nd International Workshop on Graph-Theoretic Concepts in Computer Science (WG)*, volume 1197, pages 151–165, 1996.
- 16 Jeff Erickson, Kyle Fox, and Luvsandondov Lkhamsuren. Holiest minimum-cost paths and flows in surface graphs. In *Proceedings of the 50th Annual ACM Symposium on Theory of Computing (STOC)*, pages 1319–1332, 2018. doi:10.1145/3188745.3188904.
- 17 Jittat Fakcharoenphol and Satish Rao. Planar graphs, negative weight edges, shortest paths, and near linear time. *J. Comput. Syst. Sci.*, 72(5):868–889, 2006. doi:10.1016/j.jcss.2005.05.007.
- 18 Greg N. Frederickson. Fast algorithms for shortest paths in planar graphs, with applications. *SIAM J. Comput.*, 16(6):1004–1022, 1987. doi:10.1137/0216064.
- 19 Viktor Fredslund-Hansen, Shay Mozes, and Christian Wulff-Nilsen. Truly subquadratic exact distance oracles with constant query time for planar graphs. In *Proceedings of the 32nd International Symposium on Algorithms and Computation (ISAAC)*, pages 25:1–25:12, 2021. doi:10.4230/LIPICS.ISAAC.2021.25.

- 20 Paweł Gawrychowski, Haim Kaplan, Shay Mozes, Micha Sharir, and Oren Weimann. Voronoi diagrams on planar graphs, and computing the diameter in deterministic  $\tilde{O}(n^{5/3})$  time. *SIAM J. Comput.*, 50(2):509–554, 2021. doi:10.1137/18M1193402.
- 21 Paweł Gawrychowski, Shay Mozes, Oren Weimann, and Christian Wulff-Nilsen. Better tradeoffs for exact distance oracles in planar graphs. In *Proceedings of the 29th Annual ACM-SIAM Symposium on Discrete Algorithms (SODA)*, pages 515–529, 2018. doi:10.1137/1.9781611975031.34.
- 22 Qian-Ping Gu and Gengchun Xu. Constant query time  $(1 + \epsilon)$ -approximate distance oracle for planar graphs. *Theor. Comput. Sci.*, 761:78–88, 2019. doi:10.1016/j.tcs.2018.08.024.
- 23 Ken-ichi Kawarabayashi, Philip N. Klein, and Christian Sommer. Linear-space approximate distance oracles for planar, bounded-genus and minor-free graphs. In *Proceedings of the 38th Int'l Colloquium on Automata, Languages and Programming (ICALP)*, volume 6755, pages 135–146, 2011. doi:10.1007/978-3-642-22006-7\_12.
- 24 Ken-ichi Kawarabayashi, Christian Sommer, and Mikkel Thorup. More compact oracles for approximate distances in undirected planar graphs. In *Proceedings of the 24th ACM-SIAM Symposium on Discrete Algorithms (SODA)*, pages 550–563, 2013. doi:10.1137/1.9781611973105.40.
- 25 Philip N. Klein. Preprocessing an undirected planar network to enable fast approximate distance queries. In *Proceedings of the 13th ACM-SIAM Symposium on Discrete Algorithms (SODA)*, pages 820–827, 2002. URL: <http://dl.acm.org/citation.cfm?id=545381.545488>.
- 26 Philip N. Klein. Multiple-source shortest paths in planar graphs. In *Proceedings of the 16th ACM-SIAM Symposium on Discrete Algorithms (SODA)*, pages 146–155, 2005. URL: <http://dl.acm.org/citation.cfm?id=1070432.1070454>.
- 27 Philip N. Klein, Shay Mozes, and Christian Sommer. Structured recursive separator decompositions for planar graphs in linear time. In *Proceedings of the 45th Annual ACM Symposium on Theory of Computing (STOC)*, pages 505–514, 2013. doi:10.1145/2488608.2488672.
- 28 Jakub Lacki and Piotr Sankowski. Min-cuts and shortest cycles in planar graphs in  $O(n \log \log n)$  time. In *Proceedings of the 19th Annual European Symposium on Algorithms (ESA)*, pages 155–166, 2011.
- 29 Hung Le and Christian Wulff-Nilsen. Optimal approximate distance oracle for planar graphs. In *Proceedings of the 62nd Annual IEEE Symposium on Foundations of Computer Science (FOCS)*, pages 363–374, 2021. doi:10.1109/FOCS52979.2021.00044.
- 30 R. J. Lipton and R. E. Tarjan. A separator theorem for planar graphs. *SIAM J. Appl. Math.*, 36(2):177–189, 1979.
- 31 Richard J. Lipton and Robert Endre Tarjan. Applications of a planar separator theorem. *SIAM J. Comput.*, 9(3):615–627, 1980. doi:10.1137/0209046.
- 32 Yaowei Long and Seth Pettie. Planar distance oracles with better time-space tradeoffs. In *Proceedings of the 32nd ACM-SIAM Symposium on Discrete Algorithms (SODA)*, pages 2517–2536, 2021. doi:10.1137/1.9781611976465.149.
- 33 Gary L. Miller. Finding small simple cycle separators for 2-connected planar graphs. *J. Comput. Syst. Sci.*, 32(3):265–279, 1986. doi:10.1016/0022-0000(86)90030-9.
- 34 R. Motwani and P. Raghavan. *Randomized algorithms*. Press Syndicate of the University of Cambridge, 1995.
- 35 Shay Mozes, Kirill Nikolaev, Yahav Nussbaum, and Oren Weimann. Minimum cut of directed planar graphs in  $O(n \log \log n)$  time. In *Proceedings of the 29th ACM-SIAM Symposium on Discrete Algorithms (SODA)*, pages 477–494, 2018. doi:10.1137/1.9781611975031.32.
- 36 Shay Mozes and Christian Sommer. Exact distance oracles for planar graphs. In *Proceedings of the 23rd ACM-SIAM Symposium on Discrete Algorithms (SODA)*, pages 209–222, 2012. doi:10.1137/1.9781611973099.19.
- 37 K. Mulmuley, U. Vazirani, and V. Vazirani. Matching is as easy as matrix inversion. *Combinatorica*, 7(1):105–113, 1987. doi:10.1007/BF02579206.



- 38 Yahav Nussbaum. Improved distance queries in planar graphs. In *Proceedings of the 12th International Workshop on Algorithms and Data Structures (WADS)*, pages 642–653, 2011. doi:10.1007/978-3-642-22300-6\_54.
- 39 Mikkil Thorup. Compact oracles for reachability and approximate distances in planar digraphs. *J. ACM*, 51(6):993–1024, 2004. doi:10.1145/1039488.1039493.
- 40 Christian Wulff-Nilsen. *Algorithms for planar graphs and graphs in metric spaces*. PhD thesis, University of Copenhagen, 2010.
- 41 Christian Wulff-Nilsen. Approximate distance oracles for planar graphs with improved query time-space tradeoff. In *Proceedings of the 27th ACM-SIAM Symposium on Discrete Algorithms (SODA)*, pages 351–362, 2016. doi:10.1137/1.9781611974331.CH26.